

## Direct observation of local structure deformation induced by X-ray irradiation in $\kappa$ -(BEDT-TTF)<sub>2</sub>Cu[N(CN)<sub>2</sub>]Br by X-ray fluorescence holography

$\kappa$ -(BEDT-TTF)<sub>2</sub>X, where X is an anion molecule, is a family of organic crystals that has attracted significant attention in strongly correlated electron physics [1]. It is a bandwidth-controlled Mott transition system, where pressure or molecular substitution allows the control of the strength of electron correlation. It was reported that X-ray irradiation induces permanent local defects that affect their electronic properties. In particular, it has been reported that random defects induced by irradiation enhance Anderson-type electron localization in the organic superconductor  $\kappa$ -(BEDT-TTF)<sub>2</sub>Cu[N(CN)<sub>2</sub>]Br or  $\kappa$ -Br [1,2]. Contrary to Mott metal-insulator (MI) transitions, the electron localization in Anderson insulators is a result of the interference of electron wave functions due to disorder.

Experimentally, these defects have not been directly observed. No changes were observed in diffraction images even after long irradiation. By infrared optical conductivity spectroscopy, suppression of the vibration modes associated with the C–N and C≡N bonds of the dicyanamide (DCA) molecules in the anion layer was observed in the irradiated  $\kappa$ -Br (Fig. 1(a)) [1], suggesting that these defects are limited to the anion layer. First principles calculations have shown that these can be described by the “bond-shift” (BS) model [3], where irradiation breaks C–N bonds in the DCA molecules, and a C≡N fragment connects with a N–C≡N fragment of an adjacent broken DCA molecule (Fig. 1(c)). Experimentally determining the structure of these defects will be beneficial to our understanding of strongly correlated materials.

These defects, however, are difficult to investigate using conventional X-ray techniques such as X-ray diffraction (XRD) or X-ray absorption spectroscopy. To directly probe the local structure of the defects, we employ X-ray fluorescence holography (XFH). Figure 2(a) shows the principles of XFH, where atoms of a selected element are excited by an incident X-ray and emit fluorescent X-rays, which in turn are scattered by the atoms surrounding the emitter [4]. The interference of the unscattered and scattered fluorescence can be treated as a hologram pattern, where the actual 3D picture of the scatterers around the emitter can be directly reconstructed using reconstruction algorithms. XFH has been extensively used in revealing the local structures around dopants and other defects in various functional materials [4], but work on adapting XFH for organic or protein

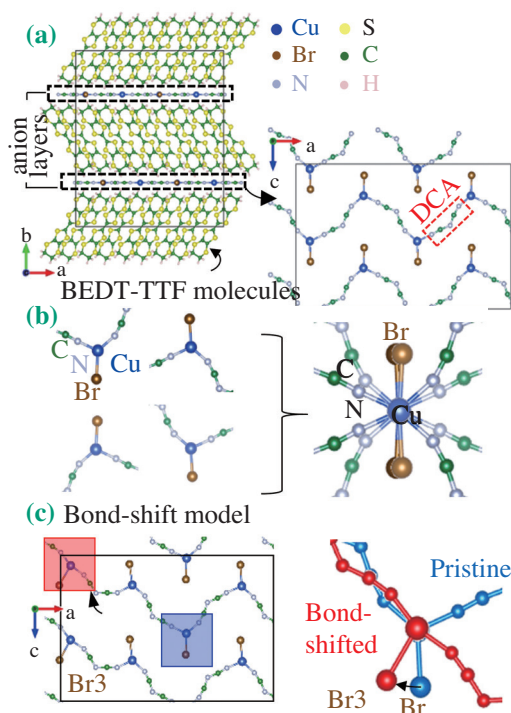


Fig. 1. (a) Atomic structure of the  $\kappa$ -Br unit cell and its anion layer, (b) the four inequivalent Cu sites, and their superposition, and (c) the “bond-shift” model proposed in Ref. 3.

crystals has only recently begun [5].

We performed XFH experiments [6] on pristine and irradiated  $\kappa$ -Br crystals at SPRING-8 BL37XU and BL39XU. In these experiments, the crystals were kept at 100 K, and diffraction patterns and resistivity measurements before and after the XFH experiments showed no additional damage due to the irradiation during the XFH experiments. Figure 2(b) shows a schematic of the bioXFH setup [5], where the fluorescent X-ray intensities were recorded as a function of the polar and azimuthal angles as the crystal was rotated relative to the incident X-ray.

From the Cu  $K\alpha$  holograms, the atomic images around Cu in the anion layers were reconstructed and are shown in Figs. 3(a) and 3(b). Atomic images coinciding with the Br positions were observed in both the pristine and irradiated samples. The nearest-neighbor N atoms were also observed as weak atomic images in the pristine sample, but were no longer visible in the irradiated crystal. Using the atomic

structures of the pristine  $\kappa$ -Br obtained by XRD, and those of the BS model from the calculations, we simulated the Cu  $K\alpha$  holograms and reconstructed the atomic images. In these simulations, the reconstruction of the pristine  $\kappa$ -Br agrees with the experiment, but for the BS model, an additional Br image appears at the Br3 position. Furthermore, the intensities of the N atomic images are far higher than those in the experiment for both models. This is because for these hologram simulations, dynamic atomic fluctuations due to thermal vibrations are not taken into account. For organic crystals, the fluctuations due to thermal vibrations are larger than those of inorganic crystals and are expected to affect the reconstructions more.

To address this, we performed molecular dynamics simulations of both the pristine and BS models at 100 K and 300 K. 150 snapshots were taken every 10 fs, where the atomic positions were taken from each frame. The Cu  $K\alpha$  holograms were calculated from these atomic positions and the atomic images were reconstructed. Figures 3(c) and 3(d) show that these reconstructions are in better agreement with the experiment. Weak N atomic images were observed in the reconstruction from the pristine model, while they are hardly visible in the BS model. Furthermore, the Br3 atomic image is no longer observed in the BS model. The MD simulations showed that the standard deviation of the angular position distribution  $\sigma_A$  at 100 K is larger for the BS model, especially for the N atoms. The large angular distribution weakens the atomic image in the reconstruction.

In summary, our results show experimental evidence supporting the BS model for explaining the MI transition in  $\kappa$ -Br, where defects in the anion layer caused by the irradiation introduce disorder in the system. Furthermore, the clear atomic images obtained from XFH experiments demonstrate that XFH can be a powerful tool in studying the local structures in functional organic crystals and even protein crystals.

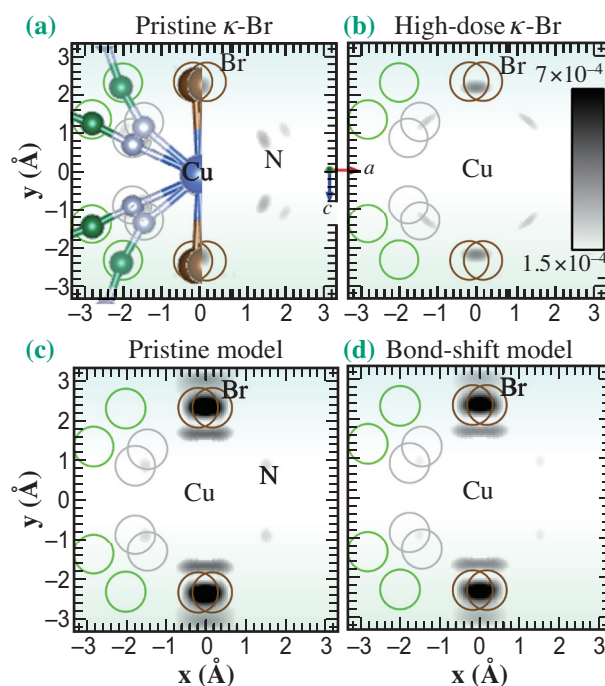


Fig. 3. Reconstructed atomic images from the experiments on the (a) pristine and (b) irradiated  $\kappa$ -Br samples and from the calculated holograms with the results from MD simulations at 100 K.

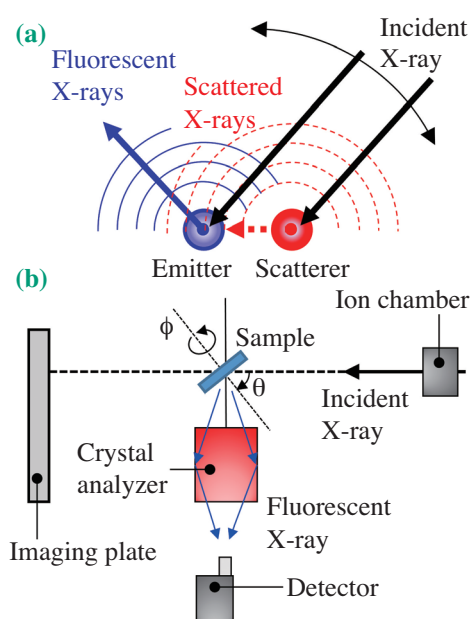


Fig. 2. (a) Principles of XFH and (b) schematic of the bioXFH experiment.

Artoni Kevin R. Ang<sup>†</sup>

Department of Physical Science and Engineering,  
Nagoya Institute of Technology

Email: ang.artoni@toyota-ti.ac.jp

<sup>†</sup> Present address: Toyota Technological Institute

### References

- [1] T. Sasaki: *Crystals* **2** (2012) 374.
- [2] K. Sano *et al.*: *Phys. Rev. Lett.* **104** (2010) 217003.
- [3] L. Kang *et al.*: *Phys. Rev. B.* **95** (2017) 214106.
- [4] K. Hayashi *et al.*: *J. Phys.: Condens. Matter.* **24** (2012) 093201.
- [5] A. Sato-Tomita *et al.*: *Rev. Sci. Instrum.* **87** (2016) 063707.
- [6] A. K. R. Ang, R. Marumi, A. Sato-Tomita, K. Kimura, N. Happo, K. Akagi, T. Sasaki and K. Hayashi: *Phys. Rev. B.* **103** (2021) 214106.